Tri-mode Capacitive Proximity Detection towards Improved Safety in Industrial Robotics

Fan Xia, Fabio Campi, *Member, IEEE*, and Behraad Bahreyni, *Senior Member, IEEE*

Abstract—**This paper presents a multi-functional capacitive sensor that is developed to improve the worker safety during the industrial human-robot interactions. The sensor is to be mounted on the worker and used to maintain a safe distance between the workers and robots or automotive parts moved by the robots. The response of a capacitive proximity sensor is a function of the distance to an object as well as the dielectric/conductance and geometry properties of the object. This uncertainty can lead to a wrong distance estimation or possibly a missed detection. The presented approach alleviates this issue by implementing three sensing capabilities including distance measurement, motion tracking, and profile recognition in a single platform. The presented sensor employs a capacitive sensing element coupled to reprogrammable interface electronics. The sensing element features a matrix of electrodes that can be reconfigured to various arrangements at run-time by controlling the interface electronics to obtain a more detailed perception of the ambient environment. Quantitative regression models are built to seek out distances while an adaptive classification tool based on support vector machines is employed to recognize the surface profiles. The performance of the sensing modalities has been experimentally assessed. Experimental results are provided to demonstrate that the system is able to detect a metallic object at distances of up to 18cm with high resolutions, track its motion, and provide an estimate for its shape.**

Index Terms—**Capacitive sensing, electrode matrix, distance measuring, parallel motion tracking, profile recognition, regression model, SVM.**

I. INTRODUCTION

THE past few decades have brought about a tremendous rise in the envisioned potential of robotic systems and a significant increase in the number of proposed applications. In the industrial area, with the increasing demand for adaptability, flexibility, and reusability, a robot-assisted but human-guided manufacturing process has proven to be superior to full automation, and hence, encouraging close cooperation between humans and machines [1]. Nevertheless, until today, there exists a notable lack in the "cooperation" between workers and robotic manipulators: the machine "intelligence" is quite limited or even unable to avoid collisions that can be dangerous to the involved humans. For years, both research [2] and

Manuscript submitted Feb 2, 2018; revised Mar 21, 2018.
F.Xia and B.Bahreyni are with School of Mechatronic Systems Engineering, Simon Fraser University, Surrey, Canada. F.Campi was with School of Engineering Science, Simon Fraser University, Burnaby, Canada.
The corresponding author is Behraad Bahreyni (behraad@ieee.org).

industrial [3] communities have strived to improve the collaboration safety. To reduce the possibility of the collisions in an unstructured environment, a safety algorithm needs to be in place to supervise the surroundings using monitoring devices to ensure safety through motion replanning or triggering of the power brakes of the robotic manipulators based on the location and trajectory of objects with unplanned routes (e.g., a human worker).

An intuitive and widely available approach is using video cameras. The location of an object is monitored in the image plane as it moves around a scene so that the trajectory of a machine can be adjusted based on this object-centric information. However, tracking objects using visual methods can be restrictive due to various reasons including the limited field of view, dependence on light intensity, partial and full object occlusions, and real-time processing requirements [4]. Although the robustness and occlusion tolerance has been improved in [5] by building a triple stereo vision system using three cameras, the cost of adding extra cameras and real-time monitoring is high. As alternatives to cameras, non-contact proximity sensors become critical components in pre-collision planners. Some of the state-of-art sensing principles of operation include infrared radiation (IR) [6], inductance [7], and capacitance [8]. Each technology has its advantages and disadvantages related to physical effect exploited for measurement. A high-performance IR proximity sensor is presented in [9], though it has 360 degrees all around sensing capability, it has problems with light-absorbing and mirroring surfaces as IR sensors rely on reflections for measurement. Inductive sensors are useful for inspection applications as they provide highly-precision measurements. However, short detection range and limited range of detectable materials prevent inductive sensors from being used where there are safety concerns. Another group of proximity detectors is capacitive sensors, which offers a cheap, robust, and flexible way of prototyping and implementing sensor systems for human-robot interaction [10]. The challenge of using capacitive sensors is they are susceptible to errors due to variations in shape, size, and material of the objects. Despite these challenges, capacitive sensing scheme offers a less expensive and reliable alternative for industrial safety objective [11].

Recently, many safety applications have been demonstrated based on capacitive proximity sensing; the measured distances are used to build warning systems [12], [13]. Despite the considerable amount of research on capacitive collision alarming systems, the study on collision avoidance under

nondeterministic conditions where robots have to sense and react to safety violations is quite limited. A close approach would be indoor positioning and human tracking [14], however, such systems tend to employ large electrodes and perform at quite low speed. Explorations on object tracking have been demonstrated previously by our group [15], [16]. This work utilizes the capacitive sensing principle and focuses on alleviating the issue of ambiguity in measurements.

This paper presents a tri-mode capacitive sensor which can provide distance measurement, parallel motion tracking, and shape recognition for industrial human-robot interaction safety applications. Instead of just detecting the presence of an object, the quantitative distance can be derived by the sensor for regulating the operation of a robot. The purpose of estimating the parallel motion trajectory is to reduce the possibility of shutting down the machine due to false alarms. Profile recognition in this proposed scenario is to classify the object into few pre-set categories, where each category stands for an object with a given shape located at a specific distance. All the functionalities are achieved with a matrix-shaped sensing architecture, which can be configured to generate multiple electric fields in order to mesh and monitor the industrial workspace. The sensory information is fused for statistical regression and Support Vector Machine (SVM) classification at the intermediate level of data processing. The developed hardware and method can also be applied to application areas outside of manufacturing safety.

This paper begins with a brief overview of the background physics and implementation of capacitive proximity sensing in Section II. This leads to Section III where a detailed explanation of the sensor operation protocol and suitable data processing methodologies are provided. Finally, evaluation results are provided in Section IV before moving to discussing and concluding remarks in Section V.

II. Capacitive Proximity Sensing

A. Capacitance Measurement

Capacitive sensing is based on the interaction between an object and an interrogating electric field which is created between a transmit electrode and a receive electrode. Smith aggregated works performed using capacitive proximity sensors at MIT Media Laboratory in the 1990s and categorized capacitive proximity sensors into three groups, namely transmit mode, transmitter loading mode, and shunt mode [17]. Among these modes, the so-called shunt mode is a three-terminal measurement, where neither the transmitter nor the receiver is in contact with the object [18]. When an object enters the electric field produced by the transmit electrode, the displacement current as well as the capacitance between transmit and receive electrodes decrease [19]. Using the shunt mode sensing, it is possible to create numerous virtual sensors while having a manageable number of electrodes based on different transmitter-receiver configurations. Moreover, the shunt mode detection can be used in combination with multiplexing methods allowing parallel accesses to multiple transmitters at the same time. An electrode matrix which can
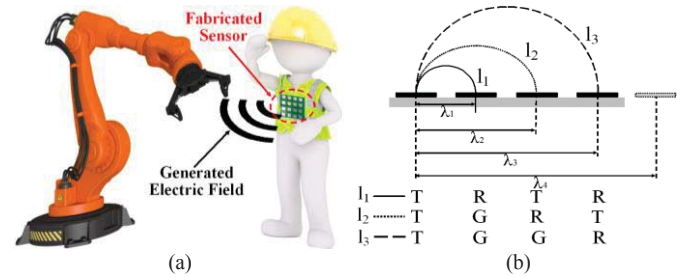

Fig. 1. (a) Sensor application diagram: sensor can be mounted either on robot side or on top of a piece of worker's garment. The electric field is generated close to the sensor to monitor the nearby environment. (b) Cross-sectional view of the electrode matrix with different penetration depth connection patterns. "T" represents the transmitter, "R" means receiver, and "G" stands for ground electrodes; l_1, l_2, l_3 represent three potential ways of connecting the electrodes.

perform various shunt mode measurements is adopted as the basic architecture of our designed capacitive proximity sensor.

Penetration depth is one of the most important figures of merit used to estimate the performance of capacitive sensors. It indicates how quickly the electric field decreases as the distance of the object to the sensor increases. Though there is no explicit formula, one way to evaluate effective penetration depth is to measure the distance at which the capacitance difference to asymptotic (i.e., sample infinitely far from the sensor) value equals to 3% of the difference between the highest and the lowest values [20]. Penetration depth is roughly proportional to the spatial wavelength λ, which is defined as the distance between the centerlines of neighboring electrode groups of the same type (e.g. transmitter or receiver).

In this work, a 2D array of electrodes are used to create different transmit/receive configurations with different penetration depths. The fabricated sensor can be mounted either on the robot side or on the worker's garment with a typical application scenario illustrated in Fig. 1 (a). The high-flexibility of our proposed matrix-structure, whose cross-sectional view is shown in Fig. 1 (b), makes it possible to arrange electrode connections in order to achieve variable penetration depths. Fig. 1 (b) illustrates that sensor penetration depth increases with larger spatial wavelength, and spatial wavelength can be easily modified by using different connection schemes in the proposed sensing system. More detailed evaluation and comparison of different electrode configurations are investigated and presented in Section IV.

B. Hardware Implementation

When designing shunt mode capacitive sensing systems, one major factor that has to be considered is the geometry. The potential electrode layouts include simple straight wires, plates, and complex multidimensional structures. More complicated structures are always optimized for specific tasks such as finger detection [21]. In the typical scenario of proximity detecting, the attention is placed on different electrode sizes, separations, and covering a large area [22]. In this work, square-shaped copper plates are used for each electrode.

The tri-mode sensor is designed to obtain information by measuring mutual capacitance between selected transmit and receive electrodes. Any pair of coplanar electrodes within the matrix can be used to generate a fringing electric field. The total
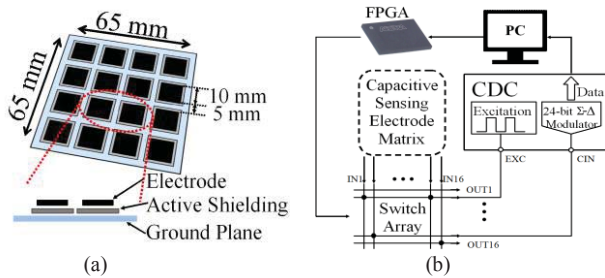
Fig. 2. Implementation of the proposed capacitive sensor. (a) The mesh structure of the electrodes and magnified cross-section view close to one electrode cell. (b) Block diagram of the sensor system for tri-mode operation.

number of independent measurements between two single electrodes is expressed as $M = N(N-1)/2$, where N is the number of electrodes. There could be more measurements when taking multiple electrodes alignments into consideration. For this work, a 4×4 electrode matrix yielding 16 independent electrodes is selected as the basic configuration. It meets the functional requirements in the context of this work with an acceptable complexity at the same time.

In principle, calculating mutual capacitance is an application of ordinary electrodynamics with impedance constraints and specific boundary conditions [23]. That makes it difficult to build a theoretical model that can respond to real measurement. An estimation given by Chen and Luo in [24] suggests that mutual capacitance is determined by geometrical parameters with the electrode separation being the most dominant one. Reducing the electrode separation results in higher sensitivity but shorter linear detection range. Whereas increasing the perimeter of each electrode has a similar effect to decreasing the separation, but with less impact. With the entire electrode matrix area being restricted to 65×65 mm² in order to fit the sensor on a piece of working garment, a combination of different spacing and separation was studied using finite element method. The size of each electrode is finally chosen as 10×10 mm² with the separation of 5 mm to achieve the best tradeoff between detection range and linearity.

One of the major limitations when utilizing capacitive-based sensors is their sensitivity to interference. Adding a backplane under the sensor substrate is proven in [25] to be helpful in avoiding the undesired detection form the back-side of the sensor. However, as the backplane is placed close to the electrodes, it forces most of the electric field to be concentrated within transmitter/receiver and itself. Consequently, capacitance changes caused by approaching objects will drop dramatically. In our design, another 4×4 electrode matrix is introduced to neutralize this side-effect. This matrix is placed in between the sensor layer and the backplane, with each electrode being driven by the same excitation signal as its corresponding electrode. This active shielding layer blocks the formation of the sensor-to-backplane parallel-plate capacitor so that the fringing electric field will be reinforced. To further enhance the isolation effect, every active shielding electrode is designed to have a slightly larger area than sensing electrode. The electrode matrix and magnified cross-section view close to the sensor cell array are depicted in Fig. 2 (a).

The sensing system is composed of a four-layer printed circuit board (PCB), a field programmable gate array (FPGA), and a capacitance-to-digital (CDC) chipset. The top three layers of the PCB serve as carriers for sensing matrix, active shielding matrix, and backplane shielding. Two analog switch matrix chips (AD75019 from Analog Devices) and required supplementary electronic components are fabricated on the bottom side. The switch chips are used to create desired connections within sensing and active shielding electrode matrix, respectively. Any or all of the switch matrices' input terminals can be programmed to connect to any or all of its output terminals [26]. This feature ensures each electrode can be independently controlled to serve as a transmitter, receiver, or ground plate. This way, various virtual capacitors can be formed to finely mesh the surrounding area. The switch matrices are controlled by the FPGA which generates timing and switching signals.

To obtain the capacitive responses, an AC signal is applied to the transmitter and the mutual capacitance is determined by measuring the displacement current on the receiver side [27]. AD7746 CDC chipset manufactured by Analog Devices is acquired to conduct a comprehensive study on capacitive sensing performance. The chip kit is used to achieve capacitance measurement, quantize the measured capacitances, and exhibit results in terms of both capacitance values and digital strings via its standard communication interface [28]. Its sampling rate is set as 90.9 Hz, which means the time consumed for one single measurement is 11 ms. Ultimately, measured data is stored and processed on an external computer. The block diagram of the system is shown in Fig. 2 (b).

III. TRI-MODE OPERATION

The designed sensor has 16 independent sensing electrodes, providing many possible configurations to generate the fringing electric field. Selecting the most suitable connection patterns for each of the functionalities plays a significant role in the application of the sensing system. Three prototypes can be implemented in the sensing matrix to cover the three application domains: distance measurement, parallel motion detection, and surface profile recognition. In this section, detailed operation protocols and corresponding data processing methodologies will be explained. Fig. 3 demonstrates all the sensing configurations used in this work in the form of matrices; each letter represents the connection of each electrode, and electrodes with the same letter are connected.

A. Operation Prototypes

Penetration depth that determines detection range is an intrinsically important factor when employing the system as a proximity sensor. Among different electrode connection patterns, three extreme configurations as illustrated in Fig. 3 (a) are chosen to compare the effect of the fringing electric field: Type I represents a comb electrode structure which generates three fringing electric fields between alternate electrode strips, whereas Type II only has one by grouping the electrodes into two equal halves [29]. In addition to these two classical structures, a third pattern Type III that utilizes only the two
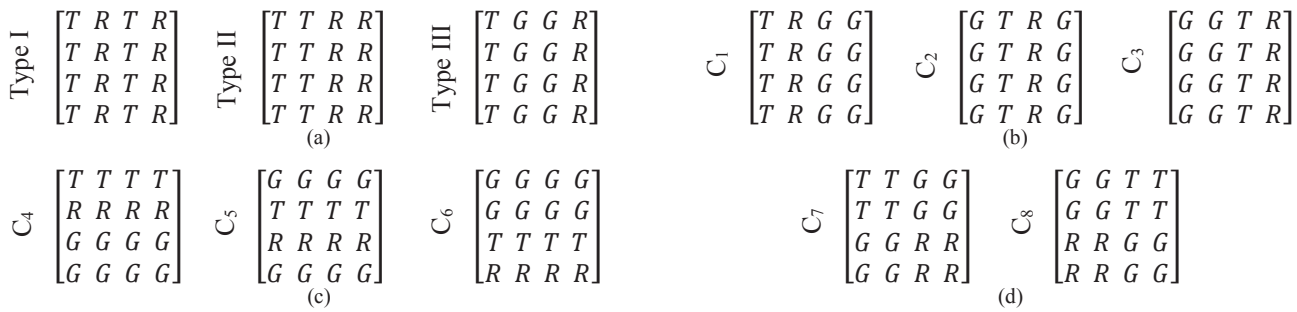
$$\text{Type I} \begin{bmatrix} T & R & T & R \\ T & R & T & R \\ T & R & T & R \\ T & R & T & R \end{bmatrix} \quad \text{Type II} \begin{bmatrix} T & T & R & R \\ T & T & R & R \\ T & T & R & R \\ T & T & R & R \end{bmatrix} \quad \text{Type III} \begin{bmatrix} T & G & G & R \\ T & G & G & R \\ T & G & G & R \\ T & G & G & R \end{bmatrix}$$

(a)

$$C_1 \begin{bmatrix} T & R & G & G \\ T & R & G & G \\ T & R & G & G \\ T & R & G & G \end{bmatrix} \quad C_2 \begin{bmatrix} G & T & R & G \\ G & T & R & G \\ G & T & R & G \\ G & T & R & G \end{bmatrix} \quad C_3 \begin{bmatrix} G & G & T & R \\ G & G & T & R \\ G & G & T & R \\ G & G & T & R \end{bmatrix}$$

(b)

$$C_4 \begin{bmatrix} T & T & T & T \\ R & R & R & R \\ G & G & G & G \\ G & G & G & G \end{bmatrix} \quad C_5 \begin{bmatrix} G & G & G & G \\ T & T & T & T \\ R & R & R & R \\ G & G & G & G \end{bmatrix} \quad C_6 \begin{bmatrix} G & G & G & G \\ G & G & G & G \\ T & T & T & T \\ R & R & R & R \end{bmatrix}$$

(c)

$$C_7 \begin{bmatrix} T & T & G & G \\ T & T & G & G \\ G & G & R & R \\ G & G & R & R \end{bmatrix} \quad C_8 \begin{bmatrix} G & G & T & T \\ G & G & T & T \\ R & R & G & G \\ R & R & G & G \end{bmatrix}$$

(d)

Fig. 3. Tri-mode operation prototypes. "T": transmitter; "R": receiver; "G": ground electrode. All the measurements are between transmitter electrodes and receiver electrodes. (a) Three configurations for distance measurement. Type I: comb electrode structure. Type II: structure consists of two large electrodes with eight copper pads per electrode. Type III: the transmitter is composed of four copper pads from one side, the receiver is made up of another four pads from the most remote side, and all the middle electrodes are grounded. (b) Electrode connections for parallel motion trajectory detection: three mutual capacitors (C_1–C_3) are formed and measured along the moving reference axis. These capacitors are also used for reconstructing the approaching object. (c) Three more mutual capacitors (C_4-C_6) along the other axis are generated for shape/location recognition. (d) Two additional capacitors (C_7-C_8) between corner electrodes are measured to promote classification accuracy.

most remote electrode strips as transmitter and receiver have also been explored. Type III is selected as a promising candidate as it generates the largest spatial wavelength λ. Capacitance responses from all of the three configurations to different object-sensor distances were measured and recorded, and quantitative analysis was performed to compare them.

More attention is paid to the movement direction in the scenario of parallel motion tracking, whereas the absolute vertical distance is of secondary interest. Thus, the trajectory history of the target object has to be analyzed continuously. In this context, parallel movement assumes an object moves parallel to a reference axis with low deviations to the other two orthogonal axes in 3-dimensional space. Electrodes are connected to four strips along the reference axis as visualized in Fig. 3 (b), and thus, three mutual capacitors between two adjacent columns can be formed. These capacitors are measured in turn periodically to scan the surroundings. Regarding the sweep detection, the interactions between the object and each capacitor would have the same shape but with certain delays in the moving direction. The parallel motion of an object can be discriminated against its past cluster centers obtained by any of the three mutual capacitors, and the moving direction can be visually recognized by combing the three sets of measurements together.

The third function supported by the same sensor is surface profile recognition. In practical applications, determining the most likely location of an object whose shape is predicted offers more value than just distinguishing different shapes. Three objects with the shape of plate, cylinder, and sphere are investigated at three separate vertical locations, and the final estimation is based on the readings of several distributed proximity sensors from the proposed electrode array. Management of electrode configurations plays an essential role in acquiring shape and distance at the same time. The key point in reconstructing desired obstacles is to distinguish the differences in terms of sensor responses among different circumstances. Electrode field between adjacent rows and adjacent columns can be generated by connecting the electrodes in a way shown in Fig. 3 (b) and (c). So that six individual capacitors are formed and the nearing space can be well meshed along two axes. Based on the surface topography,

cylinder tends to have similar capacitive responses to sphere along X-axis. To reduce this obscurity, two more capacitances between corner electrodes as depicted in Fig. 3 (d) are measured. Totally, eight sets of independent capacitances are acquired for the purpose of profile and location recognition.

B. Data Processing

Mutual capacitances representing the sensing signals are measured and quantized by the CDC chipset, and the values have to be fused and processed for desired information. Data processing is further split into raw data processing (pre-processing) stage and high-level processing stage.

The detection range and resolution of capacitive sensors are sensitive to environmental interference and have to be explored and accounted for in order to minimize the uncertainty of the result. Raw data processing is primarily intended to compensate for these non-ideal effects. One common type of interference that is added to the signal is high-frequency noises generated in the environment. Another important aspect of raw data processing is random-walk canceling. A possible cause of the drift is the impact of temperature variations on the capacitance [30]. It is essential to provide a well calibrated and adaptive baseline, which is defined as the capacitance acquired from environment without the presence of an object [31].

Both high-frequency interference and random-walk should be handled in the raw-data processing stage. A long-term measurement was carried out to monitor the intrinsic capacitance: the sensor was kept working without any approaching object for a whole week. A portion of data that consists of measured capacitance of 8 hours from a typical
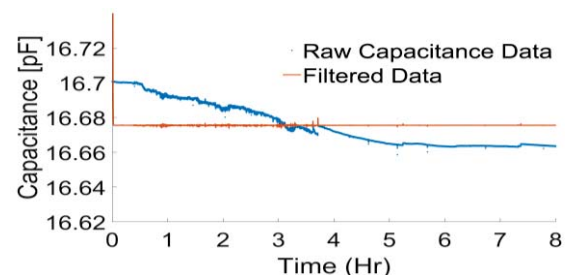
Fig. 4. Comparison of raw capacitive data from long-term measurement and filtered result

working day have been captured and plotted in Fig. 4 with blue dots. From which it can be found that the detection signal is drifting at a rather low frequency compared to the moving speed of an object whereas glitches that represent interference are at a much higher frequency. Therefore, a dc notch filter is used to cancel random-walk. Additionally, a low-pass averaging filter with the cut-off frequency 20 Hz that takes various samples in the close neighborhood and calculates an average value will be employed in this work to deal with high-frequency noise issues. The data filters are applied using Matlab and the filtered signals are plotted on the same graph in red [32]. After proper filtering, the drift issue is fully eliminated and the waveform becomes much smoother.

The ultimate goal of the designed sensor is the acquisition of information about a detectable object including its current location, its moving trend, and its shape. Statistical learning that refers to a vast set of tools for understanding data is used for high-level data processing. The information can be further characterized as either quantitative or qualitative. The distance evaluation is quantitative: the results take on numerical values. In contrast, profile recognition, which falls in one of the different shape-position categories, can be treated as a qualitative variable. The problems with a quantitative response are referred to as regression problems, while those involving a qualitative response as classification problems [33]. Different from the above two tasks, as described in operation prototypes section, parallel motion tracking is accomplished by organizing and rearrangement of the data.

Among various regression models, linear regression, which may seem dull compared to modern statistical approaches, is still an effective tool for predicting a quantitative response. Many non-linear methodologies can be treated as generalizations or extensions of linear regression. To obtain the relationship between the measured data and vertical distance, two non-linear regression models are applied and compared: high-order polynomial model and exponential model. Polynomial models are linear models that can be fitted and analyzed using linear methods. An exponential model, too, can be treated as a linear model after a transformation.

When deriving surface profile information from data, a pattern classification algorithm is used. Each of the eight measured mutual capacitances stands for one feature. All of these features are fused into one feature vector (i.e., $\{C_1, C_2, C_3, C_4, C_5, C_6, C_7, C_8\}$) for each status class that reflects both profile and location information. Feature vectors are labelled to 9 separate classes based on the distinct shape-position modes that have been investigated: plate with the distance of 5cm, 10cm, and 15cm (P@5, P@10, and P@15); cylinder with the distance of 5cm, 10cm, and 15cm (Cy@5, Cy@10, and Cy@15); and sphere with the distance of 5cm, 10cm, and 15cm (S@5, S@10, and S@15). Part of the feature vectors with their corresponding labeling information is sent to the classifier as training data, and rest of the experimental data acts as testing data for classifier performance evaluation.

As the sensing capacitance values are grouped into eight-dimensional vectors for the purpose of profile recognition, a support vector machine (SVM) with a non-linear
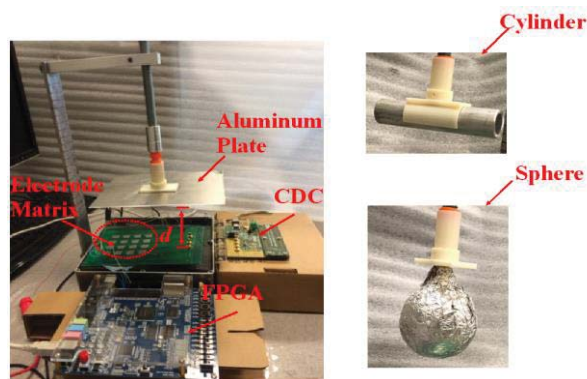

Fig. 5. Experimental setup

kernel function is employed. SVM is a classification tool which maps the features into a high-dimensional feature space and constructs a hyperplane to separate binary classes[34]. It has been for instances proven successful for robotic arm control [35] and for patient locomotion-mode identification [36]. In addition to the high-dimensional feature, SVM is chosen because it can classify accurately using nonlinear boundaries when linear boundaries are difficult to define. In this study, LIBSVM [37] which supports "one-against-one" (OAO) multiclass classification and employs N-fold cross-validation is used. The OAO strategy consists in constructing one SVM model for each pair of classes, and thus, m(m-1)/2 SVM models are created to distinguish samples of one class from another for a problem with m classes. Unknown pattern falls into the category with the maximum voting [38]. There is no clear evidence that OAO can achieve higher accuracy compared to alternative multi-class SVM methods, but Hsu and Lin claim in [39] that OAO is more practical due to its quicker training process. N-fold cross-validation procedure eliminates the overfitting issue: training vectors are randomly partitioned into N equal sized subsamples, data of one fold is used as the testing set and the remaining data is used as training data. This process is then repeated N times, with each of the N subsamples are used exactly once as validation data set. The best model is selected by the tool depending on the result.

IV. EVALUATION

In order to investigate the capabilities of the designed sensing system and to observe its behavior properties in real application scenarios, a variety of prototypical experiments are conducted. Fig. 5 shows the experimental setup and the apparatus established in this study: a height-adjustable frame is used to support different vertical positions, parallel movement, and change of shapes. The value d, which respects the vertical distance from the object to the sensor, is controlled by the positioning stage. Objects are held by a rotatable beam so that a parallel motion can be realized. The plate can be replaced by simply attaching alternative objects to the replaceable joint for surface profile classification. The three objects being used are a plate, a ball, and a cylinder. All of them are made of the aluminum. The area of the plate is 16 cm × 13cm, the diameter of the ball is 6.5 cm, and the radius and the height of the cylinder are 1.5 cm and 10 cm respectively.
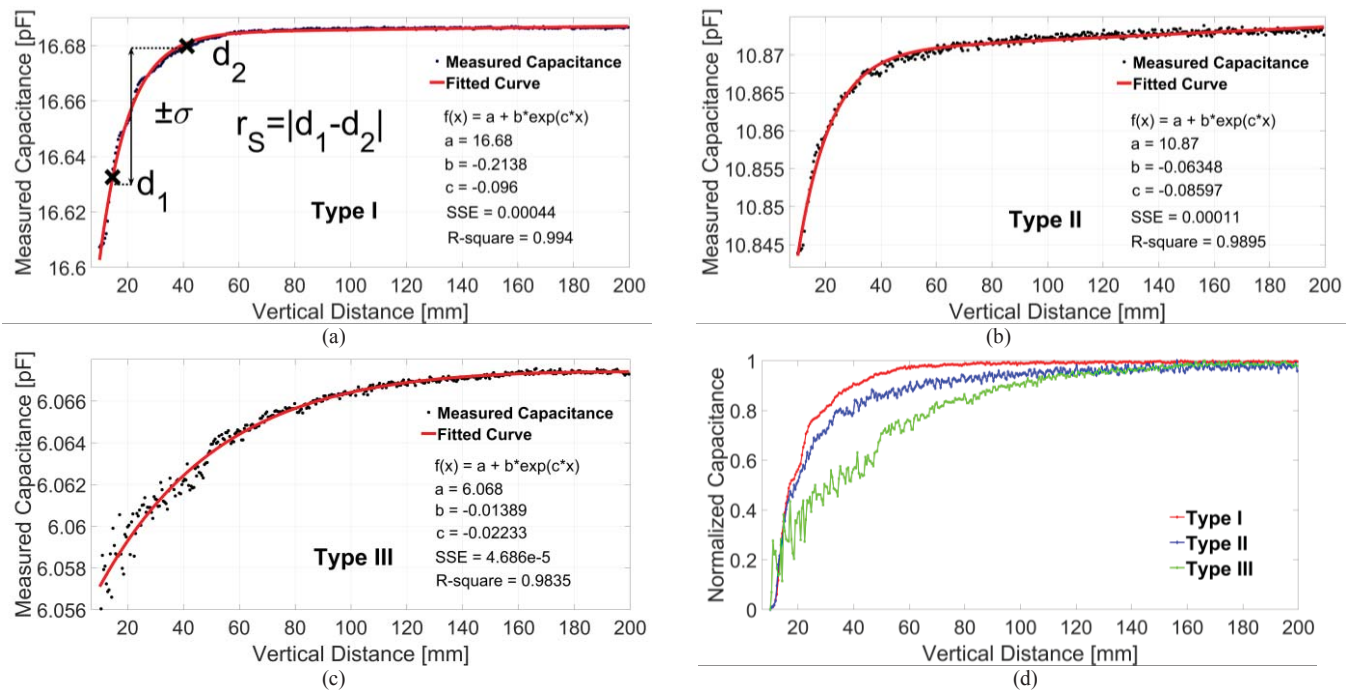
Fig. 6. (a) Measures capacitive raw data and the fitting curve for Type I. The approach to determine the spatial resolution at a given point is explained: it is based on a linearly interpolated measurement series and the standard deviation. (b) Measures capacitive raw data and the fitting curve for Type II. (c) Measures capacitive raw data and the fitting curve for Type III. (d) Normalized capacitance as a function of vertical distance for all three types.

A. Evaluation of the Proximity Sensing Capability

The proximity sensing capability is measured with respect to the electrode connection patterns: Type I, II, and III. The plate is used as the approaching object, and its vertical distance d was adjusted in successive steps from 1 cm to 20 cm.

Regression models are created to describe the mathematical relationship between a capacitive value and its corresponding distance. The original experimental samples for Type I, II, and III are plotted with black dots in Fig. 6 (a), (b), and (c) respectively. Fitted curves obtained by MATLAB curve fitting function are shown by the red lines. It can be figured out that two-term exponential regression models are able to provide high-degree of fittings. Model expressions together with corresponding coefficients and goodness indices (SSE and R-square) are also denoted in the figures. The sum of squared errors of prediction (SSE) measures the total deviation of the response values from fit values. An SSE value closer to 0 indicates the regression model has a smaller random error component and is more useful for prediction. R-square, also called the coefficient of determination, is defined as the square of the correlation between the response values and predicted values. It stands for how successful the fitting model is in terms of explaining the variation of the data, and a value closer to 1 means a greater proportion of variance is accounted for by the model. New experimental data can be inserted into the desired model and the vertical distance can be predicted by calculation.

The measured initial capacitances (at the distance of 1 cm) of Type I, II, and III are 16.607, 10.844, and 6.055 pF. Their absolute capacitive values are quite different. To enable a clear comparison in terms of sensing performances, the experimental data from these types is adjusted to a notionally common scale.

This process is known as data normalization. The method is linearly rescaling the range of data from each type to the range in [0,1]. More specifically, given the maximum capacitive value C_{max} and the lower bound C_{min} for one data set, a normalized value is calculated by $C_N = (C-C_{min})/(C_{max}-C_{min})$ to keep the values in the [0,1] range [40]. Normalized capacitance as a function of d for all the three types is represented by the colored lines in Fig. 6 (d). Though with the smallest absolute capacitance, Type III exhibits the longest linear detective range as expected whereas Type I tends to have largest capacitance change in short distance.

In order to provide a quantitative analysis of the sensing accuracy, a principle to determine a system's spatial resolution introduced in [41] is applied. The spatial resolution for a given distance d can be used as an indicator that the sensor is able to detect the defined object at this specified distance with the precision of $r_s(d)$. Type I demonstrated in Fig. 6 (a) outlines an example of obtaining spatial resolution. For each selected distance d, a series of capacitive samples are recorded for the calculation of statistical parameters. The two most important parameters are the arithmetic mean $S_n(d)$ and standard deviation $\sigma_n(d)$. The standard deviation is used to look for distances d_1 and d_2 that deviate from the mean value with $\pm\sigma_n(d)$,

TABLE I
SPATIAL RESOLUTION SUMMARY

d (mm)	$\sigma_n(d)$ (fF)			$r_s(d)$ (mm)		
	Type I	Type II	Type III	Type I	Type II	Type III
30	0.148	0.134	0.053	0.285	0.571	0.304
60	0.165	0.172	0.061	4.469	7.132	4.179
90	0.109	0.109	0.056	13.408	11.031	6.463
120	0.105	0.111	0.062	16.356	12.648	14.444
150	0.124	0.124	0.061	19.590	14.264	24.321
180	0.133	0.133	0.055	21.111	15.215	32.301

Fig. 7. Parallel motion tracking mode

Fig. 8. Horizontal actions performed by different objects at one certain distance. (a) Five different locations for the sphere. (b) The tilting positions about one central axis for the plate. There are two more along the other direction. (c) Four in-plane rotations performed by the cylinder.
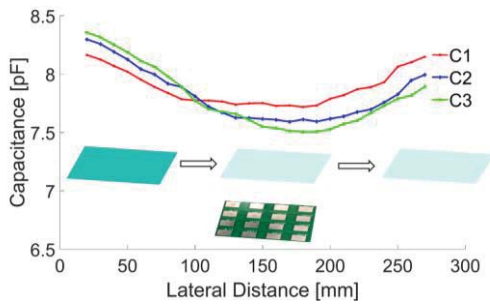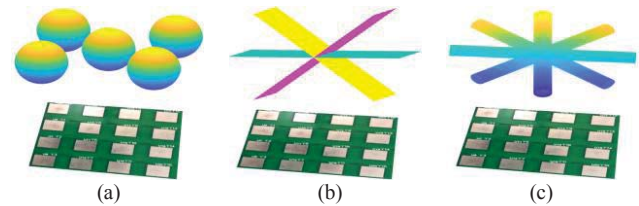
respectively. This lead to an estimation of $r_s(d)$ which is calculated as the absolute difference between d_1 and d_2. The calculated spatial resolutions for some discrete distances are summarized in Table I. The sensing precision is deteriorating with the increasing distance, as the capacitive changes are becoming small and noises have a greater influence. Type III provides a better performance in terms of resolution at short distances, whereas Type II shows better immunity to noises at long distances.

B. Parallel Motion Tracking

For tracking an object which moves in parallel with the sensor, the aluminum plate was used to simulate the parallel movement. Initially, the horizontal distance (d_H) from the center of the moveable aluminum plate to the left edge of the sensor was 10 cm with a vertical distance (d) 5 cm. Then it moved along the reference axis, which in this case is x-axis, towards until exceeded the right edge of the sensor for 10 cm. For every 1 cm of displacement, the electrode matrix was programmed to scan the three mutual capacitors (C_1, C_2, and C_3) described in Fig. 3 (b). The acquired capacitive readings along with the movement sketch are plotted in Fig. 7 with red, blue, and green dots. As can be seen, the presence of an object is detected reliably by employing any one of the three capacitors, and the moving direction can be tracked by combining all the configurations together.

C. Surface Profile Recognition

The aluminum ball, plate, and cylinder represent the three different surface profiles that are most likely to be encountered during a manufacturing process. For all subjects, capacitive measurements are performed when they are placed at three discrete vertical distances of 5 cm, 10 cm, and 15 cm. Thus, nine independent classes are formed with each class standing for one specified object appears at one certain distance.

In this task, the goal is to reliably distinguish the vertical distance together with the object's shape, whereas the horizontal status of the object is of less priority. A list of horizontal actions is executed by each object at every distance to enrich the dataset for each category. The actions being chosen for each object are appropriate metaphors for potential situations that may bring confusions to the SVM tool. The actions are also designed to make the interpretations of signals intuitively and as reproducible from time to time as possible. As a symmetrical shape, the sphere affects the sensing responds with its different horizontal locations. For every vertical distance, Fig. 8 (a) demonstrates the five relative locations that are investigated with the ball: above the center and the four corners of the sensor. On the contrast, for the plate, the most likely scenario that may cause confusions is tilting. In addition to flat position, four tilting positions are taken into consideration. Fig. 8 (b) denotes the tilting positions about one of the central axes of the plate, and there are two more along the other direction. The in-plane rotations of the cylinder could disturb the classification, so a series of rotating positions with the interval of 45° as shown in Fig. 8 (c) has been studied. Thus, the class with the shape of the sphere or the plate contains five independent data sets, whereas the class with the shape of the cylinder is made up of four datasets.

Every data is collected by performing the capacitive measurements when maintaining the subject in the desired position. Eight mutual capacitors discussed in Fig. 3 (b), (c), and (d) are measured in turns resulting in one eight-dimensional feature vector (i.e., $\{C_1, C_2, C_3, C_4, C_5, C_6, C_7, C_8\}$). Repeat this process for 100 times for collecting data sets with the ball and the plate, while for 125 times for collecting cylinder data sets. As a result, 500 feature vectors are generated for each class.

All the data inputs that contain 4500 feature vectors are labeled to 9 classes, and they are fed to LIBSVM package for model training. LIBSVM supports for multiclass classification as well as estimating class-conditional probabilities for any given feature vector. In this study, 5-fold cross-validation was employed for the training of the classifier to eliminate the overfitting issue and achieve a good compromise for bias-variance tradeoff [42]. Another series of measured data that contains 900 feature vectors with 100 from each class is acting as testing data. SVM classification accuracy, which is defined as the percentage of correctly recognized testing data out of total data, is a function of algorithm parameters β and γ. Cost parameter (β) determines various different tradeoffs between computational cost and accuracy, and gamma (γ) defines how far the influence of a single training sample
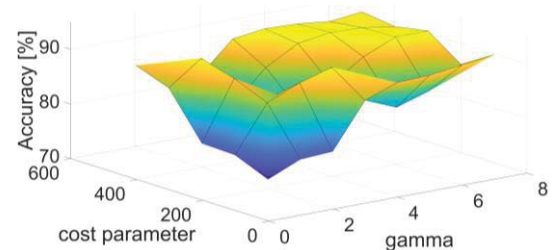

Fig. 9. Impact on classification accuracy of SVM parameters: cost parameter (β) and gamma (γ).

TABLE II
CONFUSION MATRIX FOR NINE SHAPE/DISTANCE CLASSES WITH SVM CLASSIFIER (%)

Actual class	Estimation class								
	S@5	P@5	Cy@5	S@10	P@10	Cy@10	S@15	P@15	Cy@15
S@5	95.158	0.914	1.031	0.257	0.0658	0.0547	0.217	0.0591	0.0233
P@5	0.227	46.055	38.052	5.875	0.0386	0.0328	0.0631	0.0374	0.197
Cy@5	0.165	38.820	42.923	45.900	0.0330	0.0280	0.0479	0.0322	0.0898
S@10	0.148	10.663	14.003	47.050	0.0300	0.0255	0.0451	0.0292	0.0759
P@10	0.0261	0.524	0.588	0.35	99.677	0.0026	0.0766	2.565	0.0276
Cy@10	0.0229	0.458	0.514	0.119	0.0037	99.689	0.0647	0.449	0.0240
S@15	0.159	0.733	0.824	0.190	0.0954	0.0787	99.253	0.0649	0.0082
P@15	0.0302	0.611	0.686	0.158	0.006	0.0476	0.0957	96.726	0.0317
Cy@15	4.064	1.220	1.377	0.314	0.0497	0.0416	0.134	0.0365	99.523

reaches. It is not known beforehand which β and γ could lead to the best testing result for any given problem, so a series of different parameters have been tested in this study. The impact of cost parameter and gamma on overall recognition accuracy is shown in Fig. 9. It can be observed that the overall testing accuracy is ranging from 74.67% to 90.33%, and it tends to be stable and relatively high with moderate β and γ. As larger values of β tend to consume more computational resources, the combination of β = 200 and γ = 4 was chosen for this work.

For a more comprehensive investigation of the performance of the classifier, 9 new data points, each belonging to one of the 9 classes, are provided for classification. The estimated probabilities are summarized in TABLE II, and the time consumed for one single classification is less than 0.1 ms. In most cases, surface profile together with distance information can be recognized with high confidence (more than 95% probability). However, though classifying to the correct category, the boundaries among plate at 5 cm, cylinder at 5 cm and sphere at 10 cm are ambiguous to some extent.

V. CONCLUSION

In this paper, the feasibility of a tri-mode capacitive proximity sensor for the application of industrial human-robot interaction safety has been demonstrated. The core sensor consists of a 4×4 electrode matrix which can be configured to form multiple mutual capacitors, and approaching objects can be detected by the generated shunt electric field. The three functionalities that can be achieved by the same sensing platform include vertical distance evaluation, parallel motion tracking, and surface profile recognition.

The capabilities of the proposed sensing system have been evaluated through a series of experiments, and statistical regression methods and SVM machine learning algorithm are involved to process the experimental data. Performance of different electrode connection patterns is characterized for proximity measurement. An object up to 18 cm away from the sensor can be detected with a resolution of 3cm. The surface profile together with the vertical distance can be recognized with high accuracy (95%) under a reasonable computational time (0.1s) by using LIBSVM package. The next step in this work will be cascading SVM method to obtain finer classification results.

REFERENCES

[1] J. Krüger, T. K. Lien, and A. Verl, "Cooperation of human and machines in assembly lines," *CIRP Ann. - Manuf. Technol.*, vol. 58, no. 2, pp. 628–646, 2009.

[2] S. Haddadin, A. Albu-Schäffer, and G. Hirzinger, "Requirements for Safe Robots: Measurements, Analysis and New Insights," *Int. J. Robot. Res.*, vol. 28, no. 11–12, pp. 1507–1527, Nov. 2009.

[3] B. Matthias, S. Kock, H. Jerregard, M. Källman, and I. Lundberg, "Safety of collaborative industrial robots: Certification possibilities for a collaborative assembly robot concept," in *2011 IEEE International Symposium on Assembly and Manufacturing (ISAM)*, 2011, pp. 1–6.

[4] A. Yilmaz, O. Javed, and M. Shah, "Object tracking: A survey," *ACM Comput. Surv.*, vol. 38, no. 4, p. 13–es, Dec. 2006.

[5] J. T. C. Tan and T. Arai, "Triple stereo vision system for safety monitoring of human-robot collaboration in cellular manufacturing," in *2011 IEEE International Symposium on Assembly and Manufacturing (ISAM)*, 2011, pp. 1–6.

[6] A. Rogalski, "History of infrared detectors," *Opto-Electron. Rev.*, vol. 20, no. 3, Jan. 2012.

[7] Y.-X. Guo, Z.-B. Shao, and T. Li, "An Analog-Digital Mixed Measurement Method of Inductive Proximity Sensor," *Sensors*, vol. 16, no. 1, p. 30, Dec. 2015.

[8] M. Neumayer, B. George, T. Bretterklieber, H. Zangl, and G. Brasseur, "Robust sensing of human proximity for safety applications," in *2010 IEEE Instrumentation Measurement Technology Conference Proceedings*, 2010, pp. 458–463.

[9] K. Terada *et al.*, "Development of omni-directional and fast-responsive Net-Structure Proximity Sensor," in *2011 IEEE/RSJ International Conference on Intelligent Robots and Systems*, 2011, pp. 1954–1961.

[10] D. England, Ed., *Whole Body Interaction*. London: Springer London, 2011.

[11] G. Brasseur, "Design rules for robust capacitive sensors," *IEEE Trans. Instrum. Meas.*, vol. 52, no. 4, pp. 1261–1265, Aug. 2003.

[12] N. Karlsson, "A capacitance sensor for safeguarding operators of industrial robots," *Robotica*, vol. 17, no. 01, pp. 33–39, 1999.

[13] B. George, H. Zangl, and T. Bretterklieber, "A warning system for chainsaw personal safety based on capacitive sensing," in *2008 IEEE Sensors*, 2008, pp. 419–422.

[14] M. Valtonen, J. Maentausta, and J. Vanhala, "TileTrack: Capacitive human tracking using floor tiles," in *2009 IEEE International Conference on Pervasive Computing and Communications*, 2009, pp. 1–10.

[15] F. Aezinia, Y. Wang, and B. Bahreyni, "Three dimensional touchless tracking of objects using integrated capacitive sensors," *IEEE Trans. Consum. Electron.*, vol. 58, no. 3, pp. 886–890, Aug. 2012.

[16] F. Xia, B. Bahreyni, and F. Campi, "Multi-functional capacitive proximity sensing system for industrial safety applications," in *2016 IEEE SENSORS*, 2016, pp. 1–3.

[17] J. R. Smith, "Electric field imaging," Massachusetts Institute of Technology, 1998.

[18] X. Hu and W. Yang, "Planar capacitive sensors – designs and applications," *Sens. Rev.*, vol. 30, no. 1, pp. 24–39, Jan. 2010.

[19] T. Grosse-Puppendahl and A. Braun, "Honeyfish-a high resolution gesture recognition system based on capacitive proximity sensing," in *Embedded World Conference*, 2012, vol. 12.

[20] X. B. Li, S. D. Larson, A. S. Zyuzin, and A. V. Mamishev, "Design of multichannel fringing electric field sensors for imaging. Part I. General

design principles," in *Conference Record of the 2004 IEEE International Symposium on Electrical Insulation*, 2004, pp. 406–409.

[21] G. Barrett and R. Omote, "Projected-capacitive touch technology," *Inf. Disp.*, vol. 26, no. 3, pp. 16–21, 2010.

[22] A. Braun, R. Wichert, A. Kuijper, and D. W. Fellner, "Capacitive proximity sensing in smart environments," *J. Ambient Intell. Smart Environ.*, vol. 7, no. 4, pp. 483–510, Jan. 2015.

[23] "Parallel double-plate capacitive proximity sensor modelling based on effective theory," *AIP Adv.*, vol. 4, no. 2, p. 027119, Feb. 2014.

[24] Z. Chen and R. C. Luo, "Design and implementation of capacitive proximity sensor using microelectromechanical systems technology," *IEEE Trans. Ind. Electron.*, vol. 45, no. 6, pp. 886–894, Dec. 1998.

[25] R. Pallás-Areny and J. G. Webster, *Sensors and signal conditioning*, 2nd ed. New York: Wiley, 2001.

[26] Analog Devices, "16 × 16 Crosspoint Switch Arrar," AD75019 datasheet, 2013.

[27] S. Muhlbacher-Karrer, M. Brandstotter, D. Schett, and H. Zangl, "Contactless Control of a Kinematically Redundant Serial Manipulator Using Tomographic Sensors," *IEEE Robot. Autom. Lett.*, vol. 2, no. 2, pp. 562–569, Apr. 2017.

[28] Analog Devices, "24-Bit Capacitance-to-Digital Converter with Temperature Sensor," AD7745_7746 datasheet, 2005.

[29] H. K. Lee, S. I. Chang, and E. Yoon, "Dual-Mode Capacitive Proximity Sensor for Robot Application: Implementation of Tactile and Proximity Sensing Capability on a Single Polymer Platform Using Shared Electrodes," *IEEE Sens. J.*, vol. 9, no. 12, pp. 1748–1755, Dec. 2009.

[30] A. Hoffmann, A. Poeppel, A. Schierl, and W. Reif, "Environment-aware proximity detection with capacitive sensors for human-robot-interaction," 2016, pp. 145–150.

[31] A. Braun, R. Wichert, A. Kuijper, and D. W. Fellner, "Capacitive proximity sensing in smart environments," *J. Ambient Intell. Smart Environ.*, vol. 7, no. 4, pp. 483–510, Jan. 2015.

[32] N. L. Leech and A. J. Onwuegbuzie, "An array of qualitative data analysis tools: A call for data analysis triangulation.," *Sch. Psychol. Q.*, vol. 22, no. 4, p. 557, 2007.

[33] G. James, D. Witten, T. Hastie, and R. Tibshirani, *An Introduction to Statistical Learning*, vol. 103. New York, NY: Springer New York, 2013.

[34] C. Cortes and V. Vapnik, "Support-vector networks," *Mach. Learn.*, vol. 20, no. 3, pp. 273–297, 1995.

[35] B. Crawford, K. Miller, P. Shenoy, and R. Rao, "Real-time classification of electromyographic signals for robotic control," in *AAAI*, 2005, vol. 5, pp. 523–528.

[36] H. Huang, F. Zhang, L. J. Hargrove, Z. Dou, D. R. Rogers, and K. B. Englehart, "Continuous Locomotion-Mode Identification for Prosthetic Legs Based on Neuromuscular #x2013;Mechanical Fusion," *IEEE Trans. Biomed. Eng.*, vol. 58, no. 10, pp. 2867–2875, Oct. 2011.

[37] C.-C. Chang and C.-J. Lin, "LIBSVM: a library for support vector machines," *ACM Trans. Intell. Syst. Technol. TIST*, vol. 2, no. 3, p. 27, 2011.

[38] J. Milgram, M. Cheriet, and R. Sabourin, "'One against one' or 'one against all': Which one is better for handwriting recognition with SVMs?," in *Tenth international workshop on frontiers in handwriting recognition*, 2006.

[39] C.-W. Hsu and C.-J. Lin, "A comparison of methods for multiclass support vector machines," *IEEE Trans. Neural Netw.*, vol. 13, no. 2, pp. 415–425, 2002.

[40] S. Aksoy and R. M. Haralick, "Feature normalization and likelihood-based similarity measures for image retrieval," *Pattern Recognit. Lett.*, vol. 22, no. 5, pp. 563–582, Apr. 2001.

[41] T. Grosse-Puppendahl, Y. Berghoefer, A. Braun, R. Wimmer, and A. Kuijper, "OpenCapSense: A rapid prototyping toolkit for pervasive interaction using capacitive sensing," in *2013 IEEE International Conference on Pervasive Computing and Communications (PerCom)*, 2013, pp. 152–159.

[42] G. James, D. Witten, T. Hastie, and R. Tibshirani, *An Introduction to Statistical Learning*, vol. 103. New York, NY: Springer New York, 2013.

Fan Xia received the B. S degree and the M. S degree in Microelectronics from Tianjin University, Tianjin, China, in 2011 and 2014 respectively. She is currently working towards the Ph. D degree under the supervision of Dr. Behraad Bahreyni in the Intelligent Sensing Laboratory (ISL), Simon Fraser University, Surrey, Canada. Her research interests include capacitive sensing, interface electronics, and data processing.

Fabio Campi (MSc 99, PhD 03 University of Bologna Italy) is an expert in CMOS design of ASIC, Microprocessor and embedded FPGA circuits and implementation of embedded algorithms for data transmission, encryption, classification and computation. He worked for STMicroelectronics (Agrate Brianza, Italy and Crolles, France 1999-2013) and for Menarini Silicon Biosystems (Bologna, Italy 2016-current). He has faculty member in Simon Fraser University, (Metro Vancouver, Canada, 2012-2016) teaching ASIC design, FPGA design, embedded software and RTOS. He holds 5 US and EU patents on microprocessor and embedded FPGA design and has published on 4 textbooks and over 70 papers at IEEE international conferences and magazines.

Behraad Bahreyni (SM'98, M'07, SM'14) is an Associate Professor and the founding Director of the Intelligent Sensing Laboratory (ISL) at the School of Mechatronic Systems Engineering at Simon Fraser University, BC, Canada. He received his BSc in electronics engineering from Sharif University of Technology, Iran, and MSc and Ph.D. degrees in electrical engineering from the University of Manitoba, Canada, in 1999, 2001, and 2006, respectively. He was a post-doctoral researcher with the NanoSicence Centre at Cambridge University, UK, where he conducted research on interface circuit design for microresonators. He joined Simon Fraser University in 2008 after a one-year tenure in the industry as a MEMS design engineer. Over the past decade, his research activities have focused on the design and fabrication sensing systems comprising micro/nano sensors from silicon, polymers, or nanocomposites, their interface electronics, and the required signal processing algorithms. Dr. Bahreyni is the author of more than 100 technical publications including a book on the fabrication and design of resonant microdevices.